Automated Motion Correction and 3D Vessel Centerlines Reconstruction from Non-simultaneous Angiographic Projections

Abhirup Banerjee[2,3(✉)], Rajesh K. Kharbanda[2], Robin P. Choudhury[1,2], and Vicente Grau[3]

[1] Oxford Acute Vascular Imaging Centre, Oxford, UK
[2] Radcliffe Department of Medicine, Division of Cardiovascular Medicine, University of Oxford, Oxford, UK
{abhirup.banerjee,robin.choudhury}@cardiov.ox.ac.uk
[3] Department of Engineering Science, Institute of Biomedical Engineering, University of Oxford, Oxford, UK
vicente.grau@eng.ox.ac.uk

Abstract. Automated estimation of 3D centerlines is necessary to transform angiographic projections into accurate 3D reconstructions. Although several methods exist for 3D centerline reconstruction, most of them are sensitive to the motion in coronary arteries when images are acquired by a single-plane rotational X-ray system. The objective of the proposed method is to rectify the motion-related deformations in coronary vessels from 2D projections and subsequently achieve an optimal 3D centerline reconstruction. Rigid motion in arteries is removed by estimating the optimal rigid transformation from all projection planes. The remaining non-rigid motion at end-diastole is modelled by a radial basis function based warping of 2D centerlines. Point correspondences are then generated from all projection planes by least squares matching. The final 3D centerlines are obtained by 3D non-uniform rational basis splines fitting over generated point correspondences. Experimental analysis over 20 coronary vessel trees (12 right coronary artery: RCA and 8 left coronary artery: LCA) demonstrates that the rigid transformation is able to reduce the coronary vessel movements to 0.72 mm average, while the final 3D centerline reconstruction achieves an average rms error of 0.31 mm, when backprojected on angiographic planes.

Keywords: 3D centerline reconstruction · Coronary tree · Angiograms · Motion correction · NURBS

1 Introduction

Invasive coronary X-ray arteriography (ICA) is one of the best diagnostic tools for the assessment of coronary arterial diseases, due to its high temporal and

M. Pop et al. (Eds.): STACOM 2018, LNCS 11395, pp. 12–20, 2019.
https://doi.org/10.1007/978-3-030-12029-0_2

spatial resolution [11]. However, the limitation of depicting only 2D projection images of the complex 3D anatomy makes it susceptible to artifacts (due to vessel overlap and foreshortening) and affects the accuracy of the estimation of lesion severity and stent size (due to subjective interpretation) [7]. To overcome this inherent limitation of ICA, several groups have attempted 3D reconstruction of coronary arterial (CA) trees from a limited number of 2D projections [4]. A major component of the 3D arterial tree reconstruction is the accurate estimation of the 3D vessel centerline that uses the geometrical and topological information from 2D image projections, to compute the geometry of the 3D CA tree.

One of the earliest 3D centerline reconstruction methods introduced an epipolar line based technique [9]. For each point along a vessel in the first image plane, an epipolar straight line was generated in the second plane and its intersection with the vessel axis generated the point correspondence. Despite being susceptible to the distortions due to cardiac and breathing movements, this method was applied widely in several CA tree reconstructions. Ding and Friedman [6] incorporated the method for quantification of arterial motion from biplane coronary cineangiograms. Chen and Carroll [5] determined the transformation in imaging geometry before applying the same centerline reconstruction. Their experimental analysis over 20 LCA and 20 RCA cases by comparing the projection on a third plane generated the average rms errors of 3.09 mm and 3.13 mm, respectively.

Since reconstructions using two projections have not been shown as sufficiently reliable in clinical studies up to now, Blondel et al. [1] projected the reconstructed 3D vessel points from two angiograms on the third plane to generate a score based on multiscale analysis. The final correspondence was generated by minimizing a semi-local energy function. Cañero et al. [3] calibrated the system for geometrical distortions before applying the 3D centerline reconstruction using a biplane snakes model. Along with the epipolar constraint, Mourgues et al. [12] introduced a cost on the distance to epipolar lines and a penalty to constraint the match of all bifurcations to define point correspondences between two projections. This reconstruction method was later integrated with 3D motion tracking [13] and prospective motion correction [14] in biplane angiograms.

Recently, Galassi et al. [8] have developed a nonuniform rational basis splines (NURBS) based CA reconstruction method where the 3D centreline is reconstructed as the intersection of surfaces from corresponding branches. The method identified corresponding points sampled at uniform distances on the projection lines. Another NURBS-based 3D CA tree reconstruction method is proposed in [15], where the point correspondences between two angiographic projections are identified based on a cost matrix and the geometry correction using calibration has generated average mse 2.532–3.259 mm^2 in clinical data.

Most of the existing reconstruction methods were performed on end-diastole frames of angiograms, where cardiac motion was assumed to not exist between projections. However, in a single-plane rotational X-ray system, this assumption does not hold for non-simultaneous acquisition. Single-plane systems have some advantages over biplane ones, such as their lower cost and the possibility of acquiring any number of projections. To remove the effects of respiration and

patient related movements, in previous works the cardiac images for reconstruction were mostly acquired by breath-holding and ensuring no patient movement [1,3,15]. However, breath-holding does not necessarily ensure the generation of images at the same respiratory cycle and often the patients are not in a state to follow the breath-hold protocol. Also, the assumption of no patient movement is often violated due to invasive nature of the procedure.

The purpose of the proposed research work is to generate 3D vessel centerlines from multiple angiographic projections without the need for any assumptions during image acquisition. The proposed method initially estimates optimal rigid transformations from all projection planes to remove rigid motion due to respiration and patient movements. The remaining non-rigid movements at end-diastole, mostly due to cardiac motion, are modelled by a radial basis function based warping of the 2D centerlines. Pointwise correspondences are then identified by least squares matching from all projection planes. Finally, the 3D centerlines of all coronary vessels are obtained by 3D non-uniform rational basis splines (NURBS) fitting over generated point correspondences. The method is qualitatively and quantitatively evaluated on 12 RCA and 8 LCA trees from clinical datasets.

2 Proposed Method

2.1 Rigid Motion Correction

One of the main problems with 3D reconstruction of CA tree is that acquired angiogram images from different views do not correspond to the same geometry. Even after selecting the end-diastolic frames for non-simultaneous image acquisition, the discrete selection of image frame from end-diastolic cardiac phase retains certain amount of temporal misalignment, and thus non-rigid deformations in the coronary vessels. Respiratory movements of the lungs cause rigid movement in the heart and, hence, in the vessels. Patient or device-related movements during or between image acquisitions also cause similar rigid movement.

In order to remove the effects of rigid movement due primarily to respiration and patient or device related motion, the proposed algorithm aims to estimate the optimal rigid transformations of all projection planes that minimize the rigid movement of the heart during imaging. The proposed technique models this motion by estimating the transformed location of the projection planes that optimizes the match between projections. The proposed rigid motion correction procedure requires the selection of a few (preferably 4–6) corresponding landmark points from all projection planes. In our current implementation, the bifurcation points of vessels are manually selected as landmark points.

Let us assume the motion corrected 3D locations of r landmark points are given by $B_i, i = 1, \cdots, r$ and the true location of landmark B_i on the jth projection plane is $b_{ij}, j = 1, \cdots, s$. Also, assume the location of X-ray source, origin, and normal of projection plane are defined as F_j, M_j, and $n_j, j = 1, \cdots, s$, respectively. Hence, the objective is to estimate the optimal rigid transformation (translation t_j and rotation $R_j, j = 1, \cdots, s$) from each plane, so that the

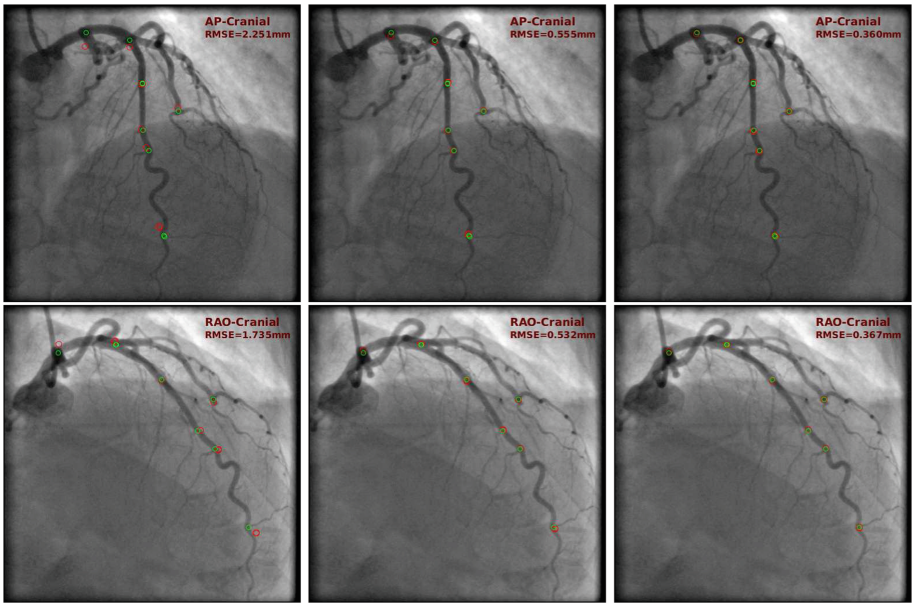

(a) Iteration 1 (b) Iteration 5 (c) At convergence

Fig. 1. Rigid-motion correction on two LCA image projections. Red and green circles in the images mark, respectively, the rigid-motion corrected and true landmark locations. (Color figure online)

projections of $B_i, i = 1, \cdots, r$ on each of the transformed angiographic planes match with the corresponding landmarks in 2D image planes, that is,

$$\min_{t_j, R_j} \sum_{i=1}^{r} \|B_{i,j'} - (t_j + R_j * b_{ij})\|^2 \quad \forall j = 1, \cdots, s. \tag{1}$$

Here, j' denotes the jth plane transformed by (t_j, R_j) and $B_{i,j'} = B_i - (n_{j'} \cdot (B_i - M_{j'})) * n_{j'}$ denotes the projection of B_i on plane j'. The optimization in (1) is solved using Horn's quaternion-based method [10]. Now, since the motion corrected 3D locations B_i are not known, these 3D landmark locations are estimated as the point of intersection of 3D straight lines $\overrightarrow{F_j b_{ij}}, j = 1, \cdots, s$, i.e.,

$$B_i = \arg\min_p \sum_j D(p; F_j, b_{ij}), \tag{2}$$

where $D(p; F_j, b_{ij}) = \|(b_{ij} - p) - ((b_{ij} - p)^T (b_{ij} - F_j))(b_{ij} - F_j)\|^2$ denotes the distance of the point p to $\overrightarrow{F_j b_{ij}}$. The minimization is solved iteratively, where, in each iteration, the 3D landmark points are generated using (2) and then projected on angiographic planes to estimate the optimal rigid transformation using (1). The algorithm usually requires 8–20 iterations to converge.

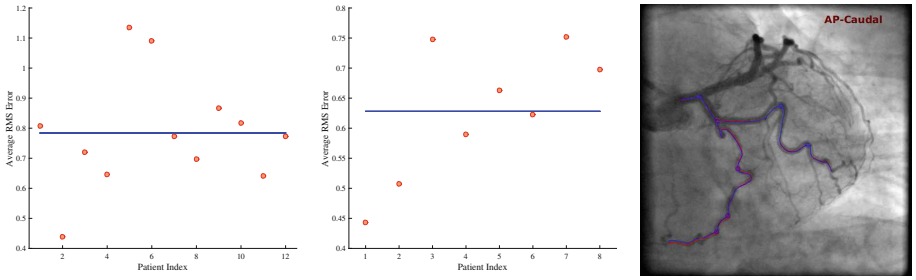

(a) RCA (b) LCA (c) Image warping

Fig. 2. (a), (b): Evaluating rigid-motion correction: red circles represent average RMSE for each patient, while blue line represents the average over all patients. (c) Modelling non-rigid motion (blue: original centerline, red: warped motion-corrected centerline). (Color figure online)

2.2 Correction of Non-rigid Motion

Although the proposed rigid motion correction can remove most of the motion artifacts from angiogram images, some amount of non-rigid motion still remains mostly around the mid-region of vessels (vessel stretching or shrinking). In order to model this non-rigid motion, the proposed work employs the radial basis function based image warping method, proposed by Bookstein [2].

Let $p_i = (x_i, y_i)$ be the true 2D coordinate of b_{ij} in the jth projection plane and $p'_i = (x'_i, y'_i)$ be the rigid-motion corrected projection of B_i in the same plane. To model the difference between p_i and p'_i due to non-rigid motion in arteries, we define, $K = ((k_{mn}))$ where $k_{mn} = \exp(-\frac{\|z_m - z_n\|^2}{r^2})$, $z_m = \|p'_m - p_m\|$, $P = [\underset{\sim}{1}, \underset{\sim}{p}]$, and $L = \begin{bmatrix} K & P \\ P^T & 0 \end{bmatrix}$. $W = L^{-1} * \underset{\sim}{p'}$ is called the coefficient matrix. Hence, the warped 2D centerline, modelling non-rigid motion at jth projection plane, is given by

$$c'_j = L^\star * W, \tag{3}$$

where c_j is the rigid-motion corrected 2D centerline, $L^\star = [K', \underset{\sim}{1}, c_j]$, $K' = ((k'_{mn}))$, $k'_{mn} = \exp(-\frac{\|z'_m - z'_n\|^2}{r^2})$, and $z'_m = \|c_j - p'_m\|$.

2.3 3D Centerline Reconstruction

After correcting rigid and non-rigid movement in the coronary vessels, point correspondences among 2D centerlines of projected planes are identified. From a 2D centerline of any of the projected planes, discrete equidistant image points (at least 250–300) are automatically selected (say, $c_{1,i}, i = 1, \cdots, n$). The corresponding locations in the remaining image planes are estimated from the optimization problem:

$$\min_{c_{j,i}; j=2,\cdots,s} \sum_{j=1}^{s} D(C_i; F_j, c_{j,i}) \quad \forall i = 1, \cdots, n \tag{4}$$

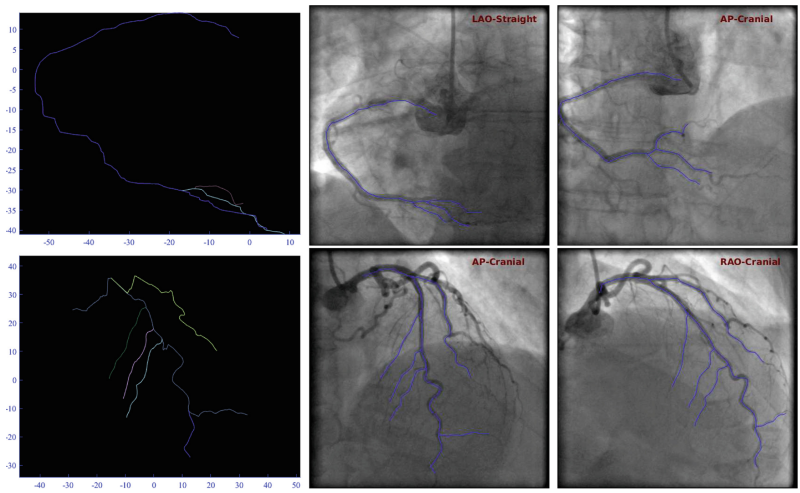

Fig. 3. From left to right: 3D centerline and back-projection of centerline on original image planes (top: RCA, bottom: LAD).

where $C_i = \arg\min_p \sum_j D(p; F_j, c_{j,i})$ and $D(\cdot)$ follows the same definition as (2). $C_i, i = 1, \cdots, n$ are estimated using the method of least squares matching, which minimizes the sum of perpendicular distances to the lines (if they do not intersect to a unique point).

Equation (4) not only identifies the point correspondences $c_{j,\cdot}$ among 2D centerlines of all projection planes, it simultaneously generates the 3D vessel points C_i. In order to produce the final 3D centerline, the 3D non-uniform rational basis splines (NURBS) function is fitted through the vessel points C_i, as follows:

$$\gamma(u) = \sum_{i=1}^{n} B_{i,p}(u) C_i, \quad u \in [0, 1], \tag{5}$$

where p is the degree of the curve and $B_{i,p}(\cdot)$ is a rational basis function of C_i of pth degree.

3 Experimental Analysis

The performance of the proposed technique is evaluated on patients enrolled in clinical studies. 12 RCA and 8 LCA images are involved in the analysis. The number of angiographic projections varied between 2 (mostly for RCA) to 5.

3.1 Motion Correction

The qualitative performance of rigid-motion correction on two LCA image projections is depicted in Fig. 1. The algorithm usually converges in 8–12 iterations

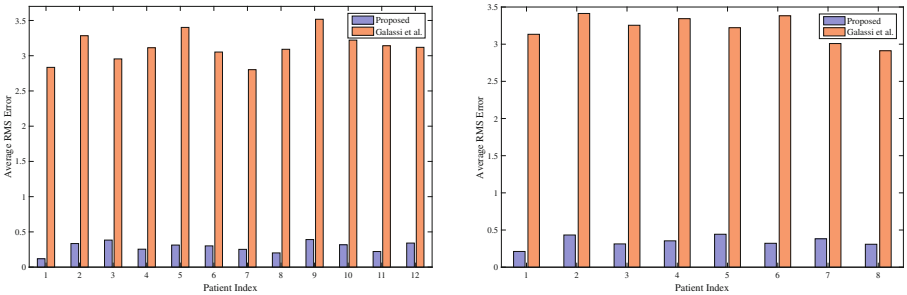

(a) Right coronary artery (b) Left coronary artery

Fig. 4. Evaluating the 3D centerline reconstruction on RCA and LCA images.

(maximum 20). The performance of the method is quantitatively evaluated by comparing the 2D locations of landmark points (in this case, bifurcation points) in each plane with the projected locations of motion-corrected 3D landmark points. For quantitative validation, we calculated the average rms error, which is presented in Fig. 2, separately for RCA and LCA. The average rms error for 12 RCA cases is 0.784 mm, while the same for 8 LCA cases is 0.628 mm. Together, the average rmse for all 20 cases is 0.7216 mm. After the rigid motion correction, the 2D centerlines of each projection plane are warped to correct the remaining non-rigid deformation, qualitatively depicted in Fig. 2(c).

3.2 3D Centerline Reconstruction

The performance of the 3D centerline reconstruction is evaluated by comparing the projected 3D centerlines on each plane with the original 2D centerlines (Fig. 3). The performance is quantitatively measured using the average rms error and presented in Fig. 4. From the results, it is observed that the proposed 3D centerline reconstruction produces average rms value 0.286 mm for 12 RCA cases and 0.346 mm for 8 LCA cases. The reconstruction performance is compared with a recently developed 3D CA reconstruction algorithm by Galassi et al. [8] (Fig. 4), showing a substantial reduction in matching error. We performed non-parametric Wilcoxon signed rank and parametric paired-t tests, both showing the improvement to be statistically significant (p-value = 2.4e−04 and 4.4e−15).

4 Discussion and Conclusions

The objective of the proposed research work is to develop a new 3D centerline reconstruction algorithm, maintaining the standard clinical image acquisition procedure, without the need for any additional constraint to reduce motion between acquisitions. The proposed approach aims at removing the effects of both rigid and non-rigid motion, so that the point correspondences can be identified for 3D centerline generation. Experimental analysis has showed that the

proposed algorithm reduces the rigid motion effects to average 0.72 mm. The performance of the final 3D centerline reconstruction shows an average rms error of 0.31 mm over 20 cases, significantly lower compared to a recent 3D reconstruction algorithm [8]. Although the proposed algorithm provides satisfactory reconstruction performance, qualitatively as well as quantitatively, at proximal and distal areas of vessels, there is scope for improvement around the middle sections of vessels, where non-rigid motions have a high impact. The future work will aim to develop new algorithms that can improve this limitation. The proposed approach is completely automated, except for the manual selection of landmark points for rigid motion correction. These landmarks were selected to correspond to clearly visible structures in the images to facilitate accurate selection. While any obvious errors arising from possible landmark inaccuracies were not detected during the analysis, a complete automation would be desirable to facilitate the clinical application of the technique.

Acknowledgments. This work was supported in part by a British Heart Foundation (BHF) Project Grant. The authors acknowledge the use of services and facilities of the Oxford Acute Vascular Imaging Centre (AVIC) and the Institute of Biomedical Engineering (IBME), University of Oxford.

References

1. Blondel, C., Vaillant, R., Devernay, F., Malandain, G., Ayache, N.: Automatic trinocular 3D reconstruction of coronary artery centerlines from rotational X-ray angiography. In: Proceedings of the 16th International Congress and Exhibition on Computer Assisted Radiology and Surgery, pp. 832–837 (2002)
2. Bookstein, F.L.: Principal warps: thin plate splines and the decomposition of deformations. IEEE Trans. Pattern Anal. Mach. Intell. **11**(6), 567–585 (1989)
3. Cañero, C., Vilariño, F., Mauri, J., Radeva, P.: Predictive (un)distortion model and 3-D reconstruction by biplane snakes. IEEE Trans. Med. Imaging **21**(9), 1188–1201 (2002)
4. Çimen, S., Gooya, A., Grass, M., Frangi, A.F.: Reconstruction of coronary arteries from X-ray angiography: a review. Med. Image Anal. **32**, 46–68 (2016)
5. Chen, S.Y.J., Carroll, J.D.: 3-D reconstruction of coronary arterial tree to optimize angiographic visualization. IEEE Trans. Med. Imaging **19**(4), 318–336 (2000)
6. Ding, Z., Friedman, M.H.: Quantification of 3-D coronary arterial motion using clinical biplane cineangiograms. Int. J. Card. Imaging **16**(5), 331–346 (2000)
7. Eng, M.H., Hudson, P.A., Klein, A.J., Chen, S.J., et al.: Impact of three dimensional in-room imaging (3DCA) in the facilitation of percutaneous coronary interventions. J. Cardiol. Vasc. Med. **1**, 1–5 (2013)
8. Galassi, F., Alkhalil, M., Lee, R., Martindale, P., et al.: 3D reconstruction of coronary arteries from 2D angiographic projections using non-uniform rational basis splines (NURBS) for accurate modelling of coronary stenoses. Plos One **13**(1), 1–23 (2018)
9. Guggenheim, N., Doriot, P.A., Dorsaz, P.A., Descouts, P., Rutishauser, W.: Spatial reconstruction of coronary arteries from angiographic images. Phys. Med. Biol. **36**(1), 99–110 (1991)

10. Horn, B.K.P.: Closed-form solution of absolute orientation using unit quaternions. J. Opt. Soc. Am. A **4**(4), 629–642 (1987)
11. Mark, D.B., Berman, D.S., Budoff, M.J., Carr, J.J., et al.: Expert consensus document on coronary computed tomographic angiography. J. Am. Coll. Cardiol. **55**(23), 2663–2699 (2010)
12. Mourgues, F., Devernay, F., Malandain, G., Coste-Manière, E.: 3D+t modeling of coronary artery tree from standard non simultaneous angiograms. In: Proceedings of the 4th International Conference on Medical Image Computing and Computer-Assisted Intervention, pp. 1320–1322 (2001)
13. Shechter, G., Devernay, F., Coste-Manière, E., Quyyumi, A., McVeigh, E.R.: Three-dimensional motion tracking of coronary arteries in biplane cineangiograms. IEEE Trans. Med. Imaging **22**(4), 493–503 (2003)
14. Shechter, G., Shechter, B., Resar, J.R., Beyar, R.: Prospective motion correction of X-ray images for coronary interventions. IEEE Trans. Med. Imaging **24**(4), 441–450 (2005)
15. Vukicevic, A.M., Çimen, S., Jagic, N., Jovicic, G., Frangi, A.F., Filipovic, N.: Three-dimensional reconstruction and NURBS-based structured meshing of coronary arteries from the conventional X-ray angiography projection images. Sci. Rep. **8**, 1711 (2018)